



## A legacy of Hadean silicate differentiation inferred from Hf isotopes in Eoarchean rocks of the Nuvvuagittuq supracrustal belt (Québec, Canada)

Martin Guitreau<sup>a,1</sup>, Janne Blichert-Toft<sup>a,\*</sup>, Stephen J. Mojzsis<sup>a,b</sup>, Antoine S.G. Roth<sup>c</sup>, Bernard Bourdon<sup>a</sup>

<sup>a</sup> Laboratoire de Géologie de Lyon, Ecole Normale Supérieure de Lyon and Université Claude Bernard Lyon 1, CNRS UMR 5276, 46 Allée d'Italie, 69007 Lyon, France

<sup>b</sup> Department of Geological Sciences, University of Colorado, UCB 399, 2200 Colorado Avenue, Boulder, CO 80309-0399, USA

<sup>c</sup> Institute of Geochemistry and Petrology, ETH Zurich, 8092 Zurich, Switzerland

### ARTICLE INFO

#### Article history:

Received 5 October 2012

Received in revised form

27 November 2012

Accepted 28 November 2012

Editor: B. Marty

Available online 10 January 2013

#### Keywords:

Lu–Hf

Sm–Nd

Hadean

Archean

Nuvvuagittuq

Isua

Amphibolite

### ABSTRACT

New Lu–Hf isotopic data for mafic and felsic rocks from the Nuvvuagittuq supracrustal belt (NSB) in northern Québec (Canada) yield an Eoarchean age of  $3864 \pm 70$  Ma consistent with both zircon U–Pb and whole-rock  $^{147}\text{Sm}$ – $^{143}\text{Nd}$  chronology, but in disagreement with ca. 4400 Ma ages inferred from the  $^{146}\text{Sm}$ – $^{142}\text{Nd}$  chronometer (O'Neil et al., 2008, 2012). The Lu–Hf result is interpreted as the mean emplacement age of the different autochthonous units of the NSB. An observed alignment of the data along a Lu–Hf “scatterchron” precludes a Hadean age for the NSB because its isotopic characteristics appear to be controlled by long-term radiogenic ingrowth. Emplacement of the NSB in the Hadean (e.g.,  $4362_{-54}^{+35}$  Ma if the decay constant of  $^{146}\text{Sm}$  of Kinoshita et al. (2012) is used with the O'Neil et al., 2008 data) should instead have caused age differences of hundreds of millions of years to manifest as strong deviations from the Lu–Hf scatterchron. Combined Lu–Hf and Sm–Nd data on the same NSB amphibolite samples (Ca-poor cummingtonite- and hornblende-bearing) define a mixing hyperbola at ca. 3800 Ma with end-member compositions representative of the compositional groups identified for these lithologies (O'Neil et al., 2011). Anomalously low  $^{142}\text{Nd}/^{144}\text{Nd}$  values relative to Bulk Silicate Earth are endemic to a group of rocks in the NSB termed “low-TiO<sub>2</sub>” amphibolites; this is attributable to an ancient multi-stage history of their mantle source. Modeling shows that the  $^{142}\text{Nd}/^{144}\text{Nd}$  deficits could have developed in response to a re-fertilization episode within a previously fractionated mantle domain at 4510 Ma.

© 2012 Elsevier B.V. All rights reserved.

### 1. Introduction

What little is known of our planet's formation and early evolution is severely limited by the fact that the terrestrial rock record appears to end around the Eoarchean–Hadean boundary at about 4 billion years ago (Bowring and Williams, 1999). Thus far, this temporal barrier has prevented direct observations of the primitive Earth based on actual rocks. Evidence from ancient detrital zircons in quartzites of the Narryer Gneiss Complex in Western Australia, however, shows that some Hadean crust lingered on into the Archean (Compston and Pidgeon, 1986; Froude et al., 1983). The ancient Australian zircons testify to the existence of an evolved felsic crust and surface conducive to the stability of liquid water (Mojzsis et al., 2001), the presence of relatively cool geothermal gradients (Hopkins et al., 2008) and oxidized mantle conditions (Trail et al., 2011), all within about

150–200 Myr after Earth formed (Harrison, 2009; Kemp et al., 2010). It should be noted that because zircons are generally prevalent in granitic rocks (e.g., Hoskin and Schaltegger, 2003), the Hadean mineral record almost certainly represents a biased sampling of a crust that was composed of a wide variety of rock types ranging in composition from ultramafic to felsic. Understanding the origin and fate of this primordial crust would greatly enhance what we know of Hadean geodynamics.

An essential complement to the Hadean zircon work has been the discovery of the anomalously high  $^{142}\text{Nd}/^{144}\text{Nd}$  isotope ratios reported from rocks collected in the Eoarchean (3770–3850 Ma) terranes of West Greenland and Western Australia (Bennett, 2007; Boyet et al., 2003; Caro et al., 2003, 2006; Rizo et al., 2011). The development of such anomalies resulted from Sm/Nd fractionation due to early silicate differentiation during the first few hundred million years of Earth history, followed by ingrowth of  $^{142}\text{Nd}$  produced by the decay of  $^{146}\text{Sm}$  ( $t_{1/2}=68$  million years; Kinoshita et al., 2012). The ca. 3800 Ma West Greenland rocks show enrichments of up to 15 ppm in  $^{142}\text{Nd}/^{144}\text{Nd}$  (expressed as positive  $\mu^{142}\text{Nd}$ ) compared to BSE. An overall 18 ppm difference in  $\mu^{142}\text{Nd}$  between Earth and chondrites reported by Boyet and

\* Corresponding author. Tel.: +33 4 72 72 84 88; fax: +33 4 72 72 86 77.

E-mail address: [jblicher@ens-lyon.fr](mailto:jblicher@ens-lyon.fr) (J. Blichert-Toft).

<sup>1</sup> Present address: Department of Earth Sciences, University of New Hampshire, James Hall, Durham, NH 03824-3589, USA.

Carlson (2005) has been ascribed to the existence of an early terrestrial magma ocean that fractionated Sm and Nd by crystallization and has remained hidden and untapped since then as a complementary enriched reservoir (Boyett et al., 2003; Chase and Patchett, 1988). Another viewpoint holds that the  $\mu^{142}\text{Nd}$  difference between BSE and chondrites instead derives from an initial suprachondritic Sm/Nd ratio for the Earth which would have been fractionated from the chondritic value; within this framework, no hidden reservoir is required to explain the difference between Earth (or BSE) and CHUR (Caro and Bourdon, 2010; O'Neil and Palme, 2008).

An important discovery was subsequently made by O'Neil et al. (2008), who found  $^{142}\text{Nd}/^{144}\text{Nd}$  ratios lower than the terrestrial standard (expressed as negative  $\mu^{142}\text{Nd}$ ) from rocks of the Nuvvuagittuq supracrustal belt (NSB) in northern Québec (Canada). These authors proposed a Hadean age for the NSB based on a positive correlation between  $^{142}\text{Nd}/^{144}\text{Nd}$  and  $^{147}\text{Sm}/^{144}\text{Nd}$ , which yielded a (revised) scatterchron age of 4388 Ma (O'Neil et al., 2012). Conversely, the long-lived  $^{147}\text{Sm}-^{143}\text{Nd}$  chronometer for the same rocks indicates an age of  $3819 \pm 270$  Ma, which is more consistent with the surrounding geology (Cates and Mojzsis, 2007, 2009; Cates et al., in press; David et al., 2002, 2009; Roth et al., in press).

To better understand the actual age of emplacement for the NSB and thereby the meaning of the coupled  $^{146,147}\text{Sm}-^{142,143}\text{Nd}$  systematics of these rocks, high-precision whole-rock Lu–Hf isotope measurements were performed on a diverse collection of supracrustal samples previously analyzed for  $^{146,147}\text{Sm}-^{142,143}\text{Nd}$  by Roth et al. (in press) and described in Cates et al. (in press). The Lu–Hf isotope data are compared to new and existing Sm–Nd results for the NSB (David et al., 2009; O'Neil et al., 2008, 2012; Roth et al., in press), to previous data for the ca. 3800 Ma Isua Supracrustal Belt (ISB) in southern West Greenland (Caro et al., 2006; Rizo et al., 2011), and to U–Pb zircon chronology and whole-rock geochemistry (Cates and Mojzsis, 2007, 2009; Cates et al., in press). The principal goal of this integrated approach was to shed new light on how and when the isotopic signatures of Hadean silicate differentiation could have formed, and how these were subsequently incorporated and preserved in the oldest terranes.

## 2. Samples and analytical techniques

The analyzed samples reported here, as well as details of the geological setting are referenced in Cates et al. (in press) and Roth et al. (in press). They comprise five hornblende amphibolites (IN05013, IN05019, IN05021, IN08019, IN08021), two cummingtonite amphibolites (IN08012, IN08044), one tonalitic gneiss (IN05028), six trondhjemitic gneisses (IN05003, IN05018, IN05022, IN05023, IN08023, IN08038), two granodioritic gneisses (IN05012, IN05015), and one fuchsitic (Cr-rich) quartzite (IN08001) from the Nuvvuagittuq locality and an adjacent (unnamed) belt also within the Inukjuak terrane (see Table 1). Whole-rock samples were crushed and powdered either at the Department of Geological Sciences of the University of Colorado at Boulder (CUB) or at ETH Zurich in agate mortars that were pre-cleaned with quartz sand and subsequently conditioned with small sample aliquots prior to powdering of the main sample mass. Splits from homogenized powders were divided for major, minor, and trace element geochemistry, and further subdivided for separate Sm–Nd and Lu–Hf isotope work at ETH Zurich and the Ecole Normale Supérieure in Lyon (ENSL), respectively. All Lu–Hf chemical separation and isotopic analysis were performed at ENSL. After dissolution in Parr bombs, Lu and Hf were separated from ca. 250 mg aliquots of whole-rock powder by ion-exchange column chromatography and measured for their isotopic compositions by MC–ICP–MS (Nu Plasma HR) according to

the procedures previously described by Blichert-Toft et al. (2002, 1997) and Blichert-Toft (2001). Lutetium and Hf concentrations were determined by isotope dilution using a >98% pure mixed  $^{176}\text{Lu}-^{180}\text{Hf}$  spike added to the samples prior to dissolution. The JMC-475 Hf standard was analyzed in alternation with the samples and the mass fractionation-corrected  $^{176}\text{Hf}/^{177}\text{Hf}$  ratio gave  $0.282156 \pm 0.000007$  ( $2\sigma$ ,  $n=15$ ) over the course of the analyses, which is identical within error to the accepted value of  $0.282163 \pm 0.000009$  (Blichert-Toft et al., 1997). Hence, no corrections were applied to the data. Total procedural blanks for Hf and Lu were less than 20 pg. Isochron calculations (ages and initial isotopic compositions) were performed using the ISOPLOT<sup>®</sup> 3.71 software package (Ludwig, 2008).

## 3. Results

### 3.1. Lu–Hf isotope systematics in the Nuvvuagittuq supracrustal belt

The Lu–Hf isotope data for the NSB samples analyzed here are listed in Table 1. For the gneiss samples,  $^{176}\text{Lu}/^{177}\text{Hf}$  ratios show a broad range from very low (0.0018) to suprachondritic (0.035). Likewise,  $^{176}\text{Hf}/^{177}\text{Hf}$  ratios range from 0.280474 for the least radiogenic tonalitic gneiss, to 0.282912 for the most radiogenic amphibolite in the sample suite. The NSB gneisses form a positive correlation in  $^{176}\text{Lu}/^{177}\text{Hf}-^{176}\text{Hf}/^{177}\text{Hf}$  space (Fig. 1) corresponding to an age of  $3864 \pm 70$  Ma and an initial  $^{176}\text{Hf}/^{177}\text{Hf}$  of  $0.280326 \pm 0.000026$ . This translates into an  $\varepsilon_{\text{Hf}}$  of  $+0.4 \pm 0.9$  when normalized to CHUR (Bouvier et al., 2008). The fuchsitic quartzite sample plots on the trend defined by both felsic and mafic lithologies, which is consistent with its mixed sedimentary origin (Cates et al., in press). Published data for the tonalite–trondhjemitic–granodiorite (TTG) whole-rock samples and zircons from the NSB reported in Guitreau et al. (2012) are also in good agreement with the new data presented here, both for the regressed initial  $^{176}\text{Hf}/^{177}\text{Hf}$  ( $0.280354 \pm 0.000035$ ) and the oldest Pb–Pb zircon ages (3770–3840 Ma).

When considered separately, the cummingtonite–amphibolite samples documented to preserve low  $^{142}\text{Nd}/^{144}\text{Nd}$  (Roth et al., in press) have a Lu–Hf age of  $3911 \pm 32$  Ma and an initial  $^{176}\text{Hf}/^{177}\text{Hf}$  of  $0.280295 \pm 0.000006$ . Hornblende–amphibolites yield an imprecise Lu–Hf age of  $4016 \pm 1200$  Ma with an initial  $^{176}\text{Hf}/^{177}\text{Hf}$  of  $0.28023 \pm 0.00075$ . The granitoid gneisses define a Lu–Hf age of  $3139 \pm 360$  Ma and an initial  $^{176}\text{Hf}/^{177}\text{Hf}$  of  $0.280369 \pm 0.000026$ . With the exception of the granitoid gneisses, the age determined by regression through all the samples, as well as the initial Hf isotopic composition determined herein, are consistent within analytical uncertainties with the separate age groups and initial  $^{176}\text{Hf}/^{177}\text{Hf}$  ratios. The Lu/Hf spread and absolute values for the felsic rocks are small (0.0018–0.0083) and, therefore, the age determined for these rocks should not be considered robust. It should also be noted that samples IN05003, IN05012, IN05018, and IN05028 were previously reported by Guitreau et al. (2012), but on different sample powders, and that the initial  $\varepsilon_{\text{Hf}}$  value differences between TTGs analyzed in this study and by Guitreau et al. (2012) are less than 1 epsilon unit (except for sample IN05028 for which the difference is 4.3 epsilon units). Since the Lu/Hf ratios are similar and very low for the two analyses of sample IN05028, we ascribe this difference to sample heterogeneity exacerbated by the fact that different powder aliquots were used in the two studies. Aside from this sample, the other Nuvvuagittuq TTG gneisses (IN05003, IN05012, and IN05018) have highly consistent Hf isotope compositions between this study and Guitreau et al. (2012). Sample IN05028 is the least radiogenic granitoid gneiss measured here, and also plots slightly below the main errorchron compared to the Guitreau et al. (2012)

**Table 1**  
Lu–Hf isotope data for samples from the Nuvvuagittuq supracrustal belt.

Sample type	Sample name	Age (Ma)	[Hf] (ppm)	[Lu] (ppm)	$^{176}\text{Lu}/^{177}\text{Hf}$	$2\sigma$	$^{176}\text{Hf}/^{177}\text{Hf}$	$2\sigma$	$^{176}\text{Hf}/^{177}\text{Hf}_{\text{in}}$	$\epsilon_{\text{Hf}}$	$\epsilon_{\text{Hf}}^{\text{in}}$ (3.8 Ga)	$\epsilon_{\text{Hf}}^{\text{in}}$ (3.8 Ga) BSE	$2\sigma$	Sample references	Latitude N	Longitude W
Amphibolite (Cummingtonite)	<b>INO8012</b>	3864	3.95	0.206	<b>0.00738</b>	2	<b>0.280854</b>	3	<b>0.280302</b>	−68.3	−0.1	−2.2	0.1	Cates et al. (in press)	58°16.826′	77°43.728′
Amphibolite (Cummingtonite)	<b>INO8044</b>	3864	1.73	0.389	<b>0.0319</b>	1	<b>0.282709</b>	15	<b>0.280325</b>	−2.7	+1.8	−0.3	0.5	Cates et al. (in press)	58°17.135′	77°43.630′
Amphibolite (Hornblende)	<b>INO5013</b>	3864	1.14	0.281	<b>0.0350</b>	1	<b>0.282912</b>	5	<b>0.280297</b>	+4.5	+1.0	−1.1	0.2	Cates et al. (in press)	58°16.710′	77°43.996′
Amphibolite (Hornblende)	<b>INO5019</b>	3864	1.27	0.303	<b>0.0337</b>	1	<b>0.282869</b>	8	<b>0.280344</b>	+3.0	+2.6	+0.5	0.3	Cates et al. (in press)	58°16.714′	77°43.943′
Amphibolite (Hornblende)	<b>INO5021</b>	3864	1.32	0.299	<b>0.0322</b>	1	<b>0.282778</b>	5	<b>0.280371</b>	−0.2	+3.5	+1.4	0.2	Cates et al. (in press)	58°16.715′	77°43.943′
Amphibolite (Hornblende)	<b>INO8019</b>	3864	2.16	0.379	<b>0.0249</b>	1	<b>0.282159</b>	4	<b>0.280293</b>	−22.1	+0.4	−1.7	0.1	Cates et al. (in press)	58°16.712′	77°43.908′
Fuchsitic quartzite	<b>INO8001</b>	3864	1.59	0.154	<b>0.0137</b>	1	<b>0.281389</b>	6	<b>0.280361</b>	−49.4	+2.3	+0.2	0.2	Cates et al. (in press)	58°16.826′	77°43.728′
TTG	<b>INO5003</b>	3864	4.64	0.0853	<b>0.00261</b>	1	<b>0.280528</b>	4	<b>0.280333</b>	−79.8	+0.8	−1.3	0.1	Cates and Mojzsis (2007)	58°16.718′	77°43.944′
TTG	<b>INO5012</b>	3864	4.34	0.0658	<b>0.00215</b>	1	<b>0.280506</b>	5	<b>0.280345</b>	−80.6	+1.2	−0.9	0.2	Cates and Mojzsis (2007)	58°16.708′	77°43.978′
TTG	<b>INO5015</b>	3864	4.71	0.0886	<b>0.00267</b>	1	<b>0.280512</b>	3	<b>0.280312</b>	−80.4	+0.0	−2.1	0.1	Cates et al. (in press)	58°17.714′	77°43.953′
TTG	<b>INO5018</b>	3864	3.14	0.0506	<b>0.00229</b>	1	<b>0.280499</b>	4	<b>0.280328</b>	−80.8	+0.6	−1.5	0.1	Cates and Mojzsis (2007)	58°16.718′	77°43.944′
TTG	<b>INO5022</b>	3864	3.64	0.0469	<b>0.00183</b>	1	<b>0.280474</b>	4	<b>0.280338</b>	−81.7	+0.9	−1.2	0.1	Cates and Mojzsis (2007)	58°16.718′	77°43.944′
TTG	<b>INO5023</b>	3864	3.72	0.0678	<b>0.00258</b>	1	<b>0.280514</b>	4	<b>0.280321</b>	−80.3	+0.3	−1.7	0.1	Cates et al. (in press)	58°17.523′	77°44.117′
TTG	<b>INO5028</b>	3864	4.17	0.244	<b>0.00831</b>	2	<b>0.280872</b>	3	<b>0.280250</b>	−67.6	−1.9	−4.0	0.1	Cates and Mojzsis (2007)	58°16.720′	77°43.915′
TTG	<b>INO8038</b>	3864	3.48	0.0561	<b>0.00229</b>	1	<b>0.280538</b>	4	<b>0.280367</b>	−79.4	+2.0	−0.1	0.1	Cates et al. (in press)	58°16.992′	72°43.585′
Amphibolite (Hornblende)	<b>INO8021</b>	3864	1.78	0.347	<b>0.0276</b>	1	<b>0.282251</b>	6	<b>0.280184</b>	−18.9	−3.4	−5.5	0.2	Cates et al. (in press)	58°20.619′	77°39.975′
TTG	<b>INO8023</b>	3660	2.84	0.0548	<b>0.00274</b>	1	<b>0.280683</b>	4	<b>0.280490</b>	−74.3	+6.0	+3.9	0.1	Cates et al. (in press)	58°20.710′	77°40.145′

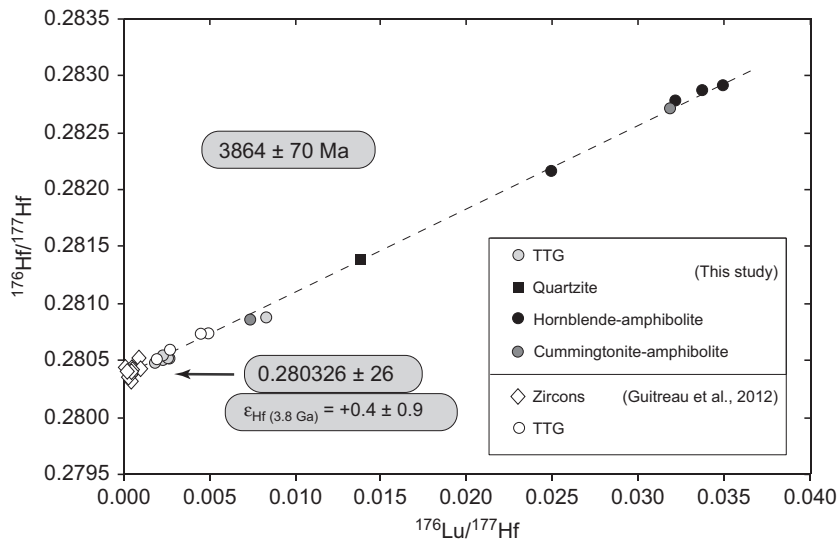


**Fig. 1.** Lu–Hf isochron diagram showing the distribution of felsic and mafic lithologies of the Nuvvuagittuq supracrustal belt from this study as well as from Guitreau et al. (2012). Analytical uncertainties on individual data points are smaller than the symbol size. Age, initial isotope composition, and uncertainties were determined using ISOPLOT<sup>®</sup> 3.71 (Ludwig, 2008) and data from this study only.

data for the same sample (Fig. 1). The apparent Lu–Hf age of 3139 Ma for the TTG gneisses is at odds with the older ca. 3800 Ga U–Pb zircon ages for the same samples, which are interpreted as crystallization ages (Cates and Mojzsis, 2007, 2009). The lack of what is normally good agreement between Hf isotopes in TTGs and their U–Pb zircon ages (Guitreau et al., 2012) means that the determined whole-rock Lu–Hf age for this subgroup of samples has no geological meaning and merely results from the very small scatter in their Lu/Hf ratios.

Initial  $^{176}\text{Hf}/^{177}\text{Hf}$  ratios calculated for an age of 3864 Ma range from 0.280250 to 0.280367 for the felsic gneisses, from 0.280293 to 0.280371 for the hornblende-amphibolites, and from 0.280302 to 0.280325 for the cummingtonite-amphibolites. Sample *IN05028* has an initial Hf isotope composition of 0.280250, while in the study of Guitreau et al. (2012) the initial was 0.280371. The quartzite has an initial  $^{176}\text{Hf}/^{177}\text{Hf}$  of 0.280361, which falls within the range defined by the other rock groups.

An age of 3800 Ma for the NSB was chosen to calculate the initial  $\epsilon_{\text{Hf}}$  (relative to CHUR; Bouvier et al., 2008). This age is used in the calculations hereafter, the reason being that it is consistent within the quoted analytical uncertainties for the long-lived chronometers applied to the same rocks (Lu–Hf, Sm–Nd, and U–Pb). In this manner, initial  $\epsilon_{\text{Hf}}$  values for the Nuvvuagittuq gneisses range from  $-1.9$  to  $+3.5$  (or from 0 to  $+3.5$  using the Guitreau et al. (2012) value for sample *IN05028*) with an average value of  $+0.4 \pm 0.9$ . This corresponds to a  $^{176}\text{Hf}/^{177}\text{Hf}$  ratio of  $0.280326 \pm 0.000026$  as given by the global scatterchron of all the samples shown in Fig. 1. When calculating relative to the BSE parameters of Caro and Bourdon (2010), it is found that initial  $\epsilon_{\text{Hf}}$  for the Nuvvuagittuq gneisses ranges from  $-4.0$  to  $+1.4$  (or from  $-2.2$  to  $+1.4$  using the Guitreau et al. (2012) value for sample *IN05028*) with an average value of  $-1.7 \pm 0.9$ .

### 3.2. Lu–Hf isotope systematics in an adjacent (unnamed) belt in the Inukjuak terrane

One of the hornblende-bearing amphibolites (*IN08021*) and one of the tonalitic gneisses (*IN08023*) analyzed in this study were sampled from a neighboring (unnamed) supracrustal belt that is part of the Inukjuak terrane and located approximately 5 km northeast of the NSB. The two samples plot somewhat off the Lu–Hf correlation line defined by the NSB rocks and yield

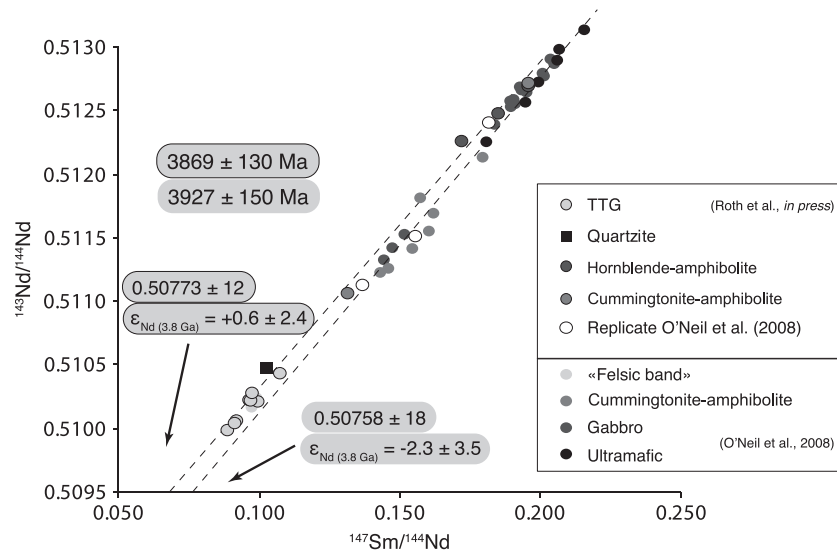
significantly different initial Hf isotope compositions when calculated using the age defined by this regression. Samples *IN08021* and *IN08023* have initial  $^{176}\text{Hf}/^{177}\text{Hf}$  calculated at 3800 Ma of 0.280219 and 0.280482, respectively, which translates into initial  $\epsilon_{\text{Hf}}$  of  $-3.4$  and  $+6.0$ . When re-calculated to the assumed age of 3660 Ma for the Voizel suite tonalites that surround the NSB (David et al., 2009), sample *IN08023* yields an initial Hf isotope composition of 0.280490. This value is significantly different from the NSB samples analyzed in this study, but resembles that determined for sample *IN05001* (0.280419) collected from a tonalite body in the center of the NSB and reported in Guitreau et al. (2012). Hence, *IN08023* may be related to the tonalitic basement that surrounds the NSB. Sample *IN08021* is petrographically and geochemically similar to common hornblende-amphibolites found in the NSB (Cates and Mojzsis, 2007; Cates et al., in press) but its age is presently unconstrained. This sample (*IN08021*) is part of a suite of rocks of great potential importance since it has among the most negative initial  $\epsilon_{\text{Hf}}$ ,  $\epsilon_{143\text{Nd}}$ , and  $\mu^{142}\text{Nd}$  (Roth et al., in press) so far observed in the Inukjuak terrane.

## 4. Discussion

### 4.1. The age(s) of the Nuvvuagittuq supracrustal belt

The actual age(s) of the NSB rocks is currently a matter of debate because of the incongruity between the two Sm–Nd chronometers (O’Neil et al., 2008; Roth et al., in press), and debate over the interpretation of U–Pb zircon ages. However, combining the two independent long-lived isotope systems (U–Pb and Lu–Hf) can help establish a robust age estimate, and consequently pave the way towards understanding the observed  $^{142}\text{Nd}$  anomalies.

Although the Lu–Hf age of 3864 Ma for the NSB determined in this study (Fig. 1) is consistent with the results of other long-lived chronometers (Cates and Mojzsis, 2007; Cates et al., in press; David et al., 2009; O’Neil et al., 2008; Roth et al., in press), it is at variance with the  $^{146}\text{Sm}$ – $^{142}\text{Nd}$  age of ca. 4400 Ma advocated by O’Neil et al. (2012). Fig. 2 shows  $^{143}\text{Nd}/^{144}\text{Nd}$  as a function of  $^{147}\text{Sm}/^{144}\text{Nd}$  for the data from Roth et al. (in press) and O’Neil et al. (2008). The Sm–Nd data for Nuvvuagittuq gneisses by David et al. (2009), that yielded an age of 3820 Ma, are not plotted in



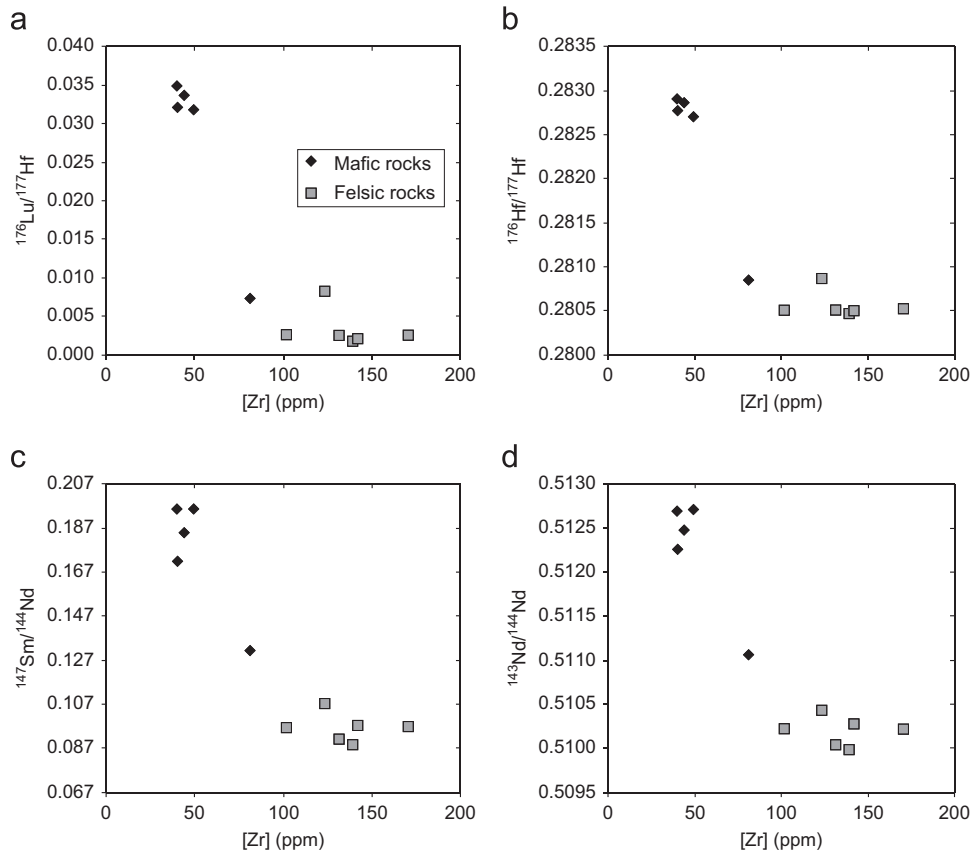
**Fig. 2.**  $^{147}\text{Sm}$ – $^{143}\text{Nd}$  isochron diagram showing the distribution of mafic and felsic lithologies of the Nuvvuagittuq supracrustal belt from previous studies (O’Neil et al., 2008; Roth et al., *in press*). Data from Roth et al. (*in press*) are the average values of dynamic measurements. Age, initial isotope compositions, and uncertainties were calculated using ISOPLOT<sup>®</sup> 3.71 (Ludwig, 2008). Black outline are results from Roth et al. (*in press*), while no outline are results from O’Neil et al. (2008). Lithology names used in this figure are identical to those of the respective publications.

Fig. 2 but they fall exactly between the two data sets. The  $^{147}\text{Sm}$ – $^{143}\text{Nd}$  ages determined by O’Neil et al. (2008), David et al. (2009), and Roth et al. (*in press*) are, respectively,  $3927 \pm 150$  Ma,  $3934 \pm 290$  Ma, and  $3869 \pm 130$  Ma. The Sm–Nd age obtained by combining the three data sets is  $3818 \pm 81$  Ma, which together with the separate ages is identical within error to the Lu–Hf age obtained in this study as well as to U–Pb zircon ages.

Evidently, after nearly four billion years in the crust, the  $^{176}\text{Hf}$  and  $^{143}\text{Nd}$  isotope systematics of these gneisses have become sufficiently dominated by radiogenic in-growth for any initial source heterogeneities to have become overwhelmed. Alternatively, the dispersion of points about the alignment of the NSB samples could be due to later metamorphic disturbance(s). Whether one or the other is the cause of the observed scatter among NSB rocks will be discussed further below (see Section 4.2.1). This conclusion does not preclude the likelihood that some of the Nuvvuagittuq rocks formed a few tens of millions of years before or after some others as hinted at by U–Pb chronology on detrital zircons (Cates et al., *in press*). However, it does rule out the possibility that the NSB rocks could have formed hundreds of millions of years earlier (or later) because this would show up as significant deviations from the observed average scatterchron. The Hadean ages derived by O’Neil et al. (2008, 2012) are dependent on the interpretation of the positive correlation between  $^{142}\text{Nd}/^{144}\text{Nd}$  and  $^{147}\text{Sm}/^{144}\text{Nd}$ . So far, no evidence of crust older than about 3800 Ma has been found in the Nuvvuagittuq detrital zircon record (Cates et al., *in press*), nor has any source of detrital zircons older than about 4000 Ma been found in North America (Maier et al., 2012). One can argue that because the NSB is dominated by amphibolites of mafic to ultramafic composition it would not be expected to contain substantial, if any, amounts of zircon. Furthermore, the apparent absence of Hadean zircons in the little-explored ancient North American detrital record is not a strong argument to refute a Hadean age for Nuvvuagittuq. Yet, as described earlier, if these rocks really were hundreds of millions of years older than the other units from the NSB, they would be expected to show real differences in the  $^{176}\text{Lu}$ – $^{176}\text{Hf}$  and  $^{147}\text{Sm}$ – $^{143}\text{Nd}$  isochron plots and would not align with the other samples.

Another line of argument may be that the  $^{147}\text{Sm}$ – $^{143}\text{Nd}$  chronometer was disturbed by metamorphism and that the 3800 Ma “age” derived from the positive correlation between  $^{143}\text{Nd}/^{144}\text{Nd}$  and  $^{147}\text{Sm}/^{144}\text{Nd}$  is merely a mixed age between ca. 4400 Ma and 2700 Ma isochrons (O’Neil et al., 2008). The latter (young) age corresponds to the formation of late zircon overgrowths (Cates and Mojzsis, 2009), and to the formation time of garnets (O’Neil et al., 2012; Sullivan et al., 2011) that are abundant in some NSB amphibolites. Garnet has a high affinity for Lu and a low partition coefficient for Hf, resulting in a mean  $^{176}\text{Lu}/^{177}\text{Hf}$  ratio in crustal garnets  $> 1$  (Duchêne et al., 1997; Herwartz et al., 2011). If these garnets were formed from exogenous metamorphic fluids, which is not a trivial issue as both internal and external fluids can be involved in metamorphism (Kohn et al., 1997), the Lu–Hf chronometer should have been significantly disturbed compared to the Sm–Nd system. This is not seen in the data. Rare-earth element (REE) patterns also would show such a disturbance, which is not observed either, and indicates that garnet mostly formed in a closed system in response to metamorphism. O’Neil et al. (2008, 2012) have also argued that the 3800 Ma age given by the  $^{147}\text{Sm}$ – $^{143}\text{Nd}$  system may have been due to a small shift in the Sm/Nd ratios that did not affect the  $^{146}\text{Sm}$ – $^{142}\text{Nd}$  age. It seems fortuitous then that the Lu–Hf system, also disturbed by metamorphism, would yield exactly the same age. The explanations provided by O’Neil et al. (2008, 2012) for the discordance between  $^{147}\text{Sm}$ – $^{143}\text{Nd}$  and  $^{146}\text{Sm}$ – $^{142}\text{Nd}$  are in contradiction with the Lu–Hf isotope results.

Recently, O’Neil et al. (2012) reported on a group of Nuvvuagittuq amphibolites that give a  $^{147}\text{Sm}$ – $^{143}\text{Nd}$  isochron age of  $4272 \pm 150$  Ma and a  $^{146}\text{Sm}$ – $^{142}\text{Nd}$  age of  $4403^{+14}_{-17}$  Ma; the two ages are consistent within analytical uncertainties. However, the sole criterion used to select the best preserved rocks that define these ages is depleted mantle model ages with  $T_{\text{DM}}$  between 4200 and 4400 Ma. A sample described by the authors as “the least disturbed” was actually rejected in their analysis because it was not isochronous between the two Sm–Nd chronometers. Without this sample an even better agreement is obtained between the  $^{147}\text{Sm}$ – $^{143}\text{Nd}$  and  $^{146}\text{Sm}$ – $^{142}\text{Nd}$  systems with ages now of, respectively,  $4321 \pm 160$  Ma and  $4406^{+14}_{-17}$  Ma. It is noteworthy that these ages are defined by only nine samples selected from the pool of



**Fig. 3.** Diagrams showing the distribution of mafic and felsic lithologies as a function of Zr contents in ppm for (a)  $^{176}\text{Lu}/^{177}\text{Hf}$  (b)  $^{176}\text{Hf}/^{177}\text{Hf}$  (c)  $^{147}\text{Sm}/^{144}\text{Nd}$  (d)  $^{143}\text{Nd}/^{144}\text{Nd}$ . The Lu–Hf data are from this study and the Sm–Nd data are from Roth et al. (in press). Note the similar data distribution between diagrams (a) and (b) and diagrams (c) and (d), which indicates that the present-day Hf and Nd isotope compositions are dominated by radiogenic ingrowth.

56 amphibolites that form the overall correlation between  $^{142}\text{Nd}/^{144}\text{Nd}$  and  $^{147}\text{Sm}/^{144}\text{Nd}$  for the NSB.

Taking all the evidence together, we consider the filtering approach of O’Neil et al. (2012) to be problematic and that 3800 Ma is the best age estimate for the emplacement time of the NSB rocks. This is because of its consistency with the Sm–Nd, Lu–Hf and U–Pb isotope systematics cited above. In the following sections, we explore how the varying age results for the NSB derived from the different short- and long-lived chronometers can be reconciled.

#### 4.2. Significance of the $^{142}\text{Nd}$ anomalies in light of U–Pb and Lu–Hf chronology

If 3800 Ma is taken as the emplacement age for the NSB (Section 3.1), interesting implications arise for the significance of anomalous  $^{142}\text{Nd}/^{144}\text{Nd}$  signatures. By this late time in Earth history, such anomalies could not have formed by radiogenic ingrowth within the rocks themselves because the parent  $^{146}\text{Sm}$  was already extinct well before 4200 Ma. In this case the anomalous ratios must have been inherited from a Hadean source or contaminant (Roth et al., in press). As discussed by O’Neil et al. (2008, 2012), the central argument in favor of a Hadean age for the NSB has been the correlation between  $^{142}\text{Nd}/^{144}\text{Nd}$  and  $^{147}\text{Sm}/^{144}\text{Nd}$ . This correlation can, however, be interpreted as a mixing line instead of an isochron. Like the positive anomalies reported for rocks in the ISB, the negative anomalies in the NSB could have been inherited from their mantle sources or derived from a crustal source. It is also possible that they originate from mantle-derived material that defines a mantle isochron; this seems to be the case for samples from the Isua supracrustal belt

(Caro, 2011) even though  $^{142}\text{Nd}/^{144}\text{Nd}$  and Sm/Nd are not as well correlated there as in Nuvvuagittuq (Roth et al., in press).

There are compelling reasons to assume that the  $^{146}\text{Sm}$ – $^{142}\text{Nd}$  system records a mixing event. Although  $^{146}\text{Sm}$  was already extinct well before NSB emplacement in the Eoarchean, the long-lived  $^{147}\text{Sm}$ – $^{143}\text{Nd}$  and  $^{176}\text{Lu}$ – $^{176}\text{Hf}$  chronometers could still form a positive correlation and therefore provide an age close to the true crystallization age because their present-day Hf and Nd isotope variations are dominated by radiogenic ingrowth. The short-lived  $^{146}\text{Sm}$ – $^{142}\text{Nd}$  chronometer evolved so rapidly while it was alive that the Hadean crust contaminant would have had a  $\mu^{142}\text{Nd}$  value well below that of the BSE. In such a case it would be highly resolvable in the mixture. This would not necessarily be the case for the long-lived Sm–Nd and Lu–Hf chronometers, especially after billions of years of radiogenic accumulation subsequent to the mixing event. To explore this further, we examined the relationships between the Lu–Hf and Sm–Nd couples, as well as their relationships with other high-field-strength elements (HFSE) and REE. The latter are relatively insensitive to alteration and metamorphism and are good tracers of both magmatic and mixing processes.

##### 4.2.1. Relationship between the Lu–Hf and Sm–Nd isotope systems

When present-day Hf isotope compositions and  $^{176}\text{Lu}/^{177}\text{Hf}$  ratios of all NSB rocks are plotted against Zr content (used here as an indicator of enrichment), it appears that the Lu–Hf distribution vs. Zr content follows the parent/daughter ratio with Hf isotope variations being fully controlled by radiogenic ingrowth (Fig. 3). This relationship also holds true for the  $^{147}\text{Sm}$ – $^{143}\text{Nd}$  system.

Another observation is that when  $\varepsilon_{\text{Hf}}$  is plotted as a function of  $\varepsilon_{\text{Nd}}$  at 3800 Ma (considered as initial values) for the amphibolite

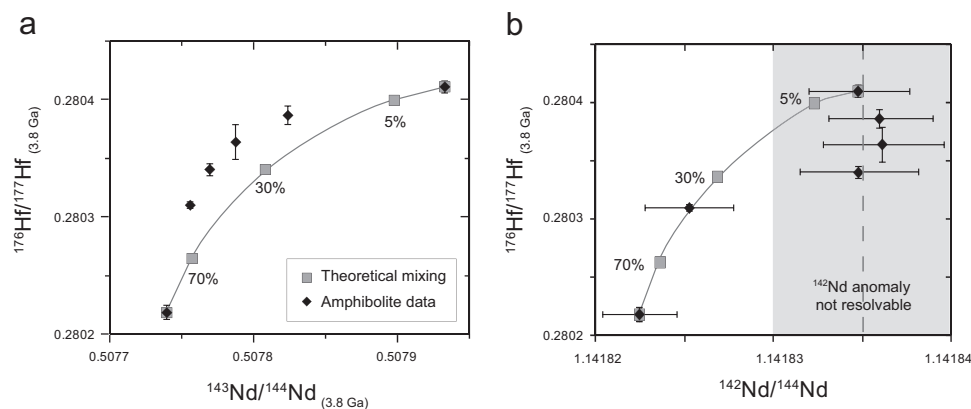


**Fig. 4.** Hafnium and  $^{143-142}\text{Nd}$  isotope plots for initial compositions of Nuvvuagittuq amphibolites calculated at 3800 Ma (black diamonds). Panel (a) shows a well-defined mixing hyperbola between  $^{176}\text{Hf}/^{177}\text{Hf}$  and  $^{143}\text{Nd}/^{144}\text{Nd}$  also seen in panel (b) showing a less well defined hyperbola between  $^{176}\text{Hf}/^{177}\text{Hf}$  and  $^{142}\text{Nd}/^{144}\text{Nd}$ . The Nd isotope data are from Roth et al. (in press). Also shown are the calculated results for variable degrees of theoretical mixing between the two extreme amphibolite compositions (grey squares) assuming they represent the two end-members.

samples only, a mixing hyperbola emerges from the data (Fig. 4a). The samples plot along a mixing curve and amphibolite sample *IN08023* (Section 3.2) coherently plots on the hyperbola with a composition that corresponds to the unradiogenic end-member. The same hyperbola also exists between Hf isotopes and  $^{142}\text{Nd}/^{144}\text{Nd}$  (Fig. 4b). As a consequence, we can infer that these relationships reflect initial source heterogeneities from likely non-cogenetic rocks.

#### 4.2.2. A mixing model for the NSB source

The well-defined hyperbola that appears from the data in Hf–Nd isotope space in Fig. 4 favors the hypothesis that the  $^{142}\text{Nd}$  anomalies were inherited from the mixing of two distinct reservoirs which gave rise to the protoliths of the NSB amphibolites. One was an enriched reservoir that carried the low  $^{142}\text{Nd}/^{144}\text{Nd}$  anomalies, and the other was a normal BSE-like reservoir. To identify likely geological candidates for the end-member reservoirs, both isotopic and elemental parameters must be considered. Two plausible geological scenarios that can account for the data are considered here: (1) interaction of two NSB magmas, with one originating from an enriched mantle reservoir with low  $^{142}\text{Nd}/^{144}\text{Nd}$ ; and (2) assimilation of ancient preserved enriched felsic Hadean crust or sub-continental lithospheric mantle. The question is whether the Nuvvuagittuq rocks were sourced from a normal BSE mantle without a  $^{142}\text{Nd}$  anomaly and then subsequently experienced contamination by an enriched reservoir carrying a low  $^{142}\text{Nd}/^{144}\text{Nd}$  signature, or whether they tapped two distinct mantle domains (including one with a negative  $^{142}\text{Nd}$  anomaly) which then subsequently commingled? The enriched end-member  $^{143}\text{Nd}/^{144}\text{Nd}$  value on the mixing hyperbola is close to 0.50773 (Fig. 4a), which is not only the asymptote on the x-axis of the covariant plot but also the initial composition deduced from the regression line through the Roth et al. (in press) data in  $^{143}\text{Nd}/^{144}\text{Nd}$ – $^{147}\text{Sm}/^{144}\text{Nd}$  space. Although the  $^{176}\text{Hf}/^{177}\text{Hf}$  composition of this contaminant is undefined, the chemistries of the amphibolite groups provide some clues.

O’Neil et al. (2011) and Cates et al. (in press) defined different amphibolite groups (“low-” and “high- $\text{TiO}_2$ ”) based on their bulk major element compositions. The mafic protoliths of these populations were necessarily sourced in two distinct mantle domains and the least and the most radiogenic of the amphibolite samples reported here belong to the “low-” and the “high- $\text{TiO}_2$ ” groups, respectively. End-members of the Hf–Nd mixing hyperbola could correspond to these two magma series. When the mixing hypothesis is tested, it is found that the calculated mixing hyperbola follows the data (Fig. 4). The curvature of the hyperbola is

determined by dividing the ratios of the respective denominators of each end-member (Langmuir et al., 1978), i.e.,

$$\left(\frac{^{177}\text{Hf}}{^{144}\text{Nd}}\right)_2 / \left(\frac{^{177}\text{Hf}}{^{144}\text{Nd}}\right)_1 \quad \text{and thus,} \quad \left(\frac{\text{Hf}}{\text{Nd}}\right)_2 / \left(\frac{\text{Hf}}{\text{Nd}}\right)_1.$$

Accordingly, the absolute concentrations of Hf and Nd in the samples strongly affect the curvature of the mixing hyperbola. The “low- $\text{TiO}_2$ ” amphibolites *IN08023* and *IN08012*, which are also the least radiogenic in our sample set, have approximately five times more Nd and four times more Sm, respectively, than the other amphibolites. The Lu and Hf concentrations are not very different among the various amphibolites, and taken together this explains well the observed curvature. Upon mixing, the Nd isotope composition of the “high- $\text{TiO}_2$ ” magmas will be rapidly dominated by that of the “low- $\text{TiO}_2$ ” magmas, whereas the Hf isotopes will change more progressively. Blichert-Toft et al. (1992) showed that predicted mixing hyperbolae do not necessarily match the natural observations as differences in element diffusion rates can create some deviation from the theoretical mixing curve.

The two samples from the hyperbola that belong to the “low- $\text{TiO}_2$ ” group both carry negative  $^{142}\text{Nd}$  anomalies, while the others belonging to the “high- $\text{TiO}_2$ ” group do not have a resolvable anomaly (data from Roth et al. (in press)). Negative correlations that exist between  $\mu^{142}\text{Nd}$  anomalies and HFSE (Zr, Hf, Ta, Nb, and  $\text{TiO}_2$ ), U, Th, and REE (except for Eu) contents for the various NSB amphibolites reported in O’Neil et al. (2008) show that the depleted and enriched “low- $\text{TiO}_2$ ” sub-groups form a continuum (Fig. 5). This is also apparent in the cordierite-anthophyllite sub-group that these authors identified (O’Neil et al., 2011), which is perhaps indicative of recrystallization of the “low- $\text{TiO}_2$ ” cummingtonite- and hornblende-amphibolite series under relatively lower pressure and/or temperature metamorphic conditions than the cordierite-anthophyllite sub-group (e.g., Abati and Arenas, 2005). The LREE enrichments of the “low- $\text{TiO}_2$ ” amphibolites are in conjunction with increasing  $^{142}\text{Nd}$  anomalies (Fig. 6a), and a positive correlation exists between  $^{142}\text{Nd}$  anomalies and  $^{147}\text{Sm}/^{144}\text{Nd}$  (Fig. 6b). The mafic end-member of the mixing hyperbola, represented by the “high- $\text{TiO}_2$ ” group amphibolites (Fig. 6c), is close to an ultramafic composition because correlations between  $\mu^{142}\text{Nd}$  and Zr, as well as Hf, predict concentrations of  $< 17$  ppm Zr and  $< 0.6$  ppm Hf for BSE (corresponding to a  $\mu^{142}\text{Nd}$  value equal to zero; Fig. 5b). Such compositions resemble ultramafic magmas such as komatiites (Arndt, 2008). Ultramafic rocks with flat REE patterns

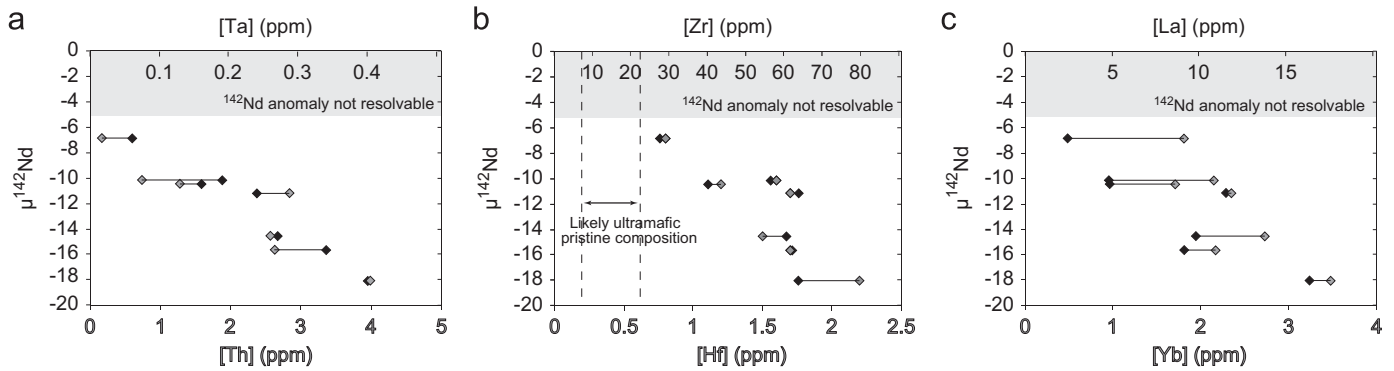


**Fig. 5.**  $^{142}\text{Nd}$  anomalies as a function of (a and b) HFSE and (c) REE contents. Data are from O'Neil et al. (2008) and correspond to the low- $\text{TiO}_2$  groups (depleted and enriched) only. Note the relatively good correlation between anomalies and element concentrations indicative of a continuum between these two low- $\text{TiO}_2$  sub-groups. Also reported in panel b is the range of likely Hf and Zr concentrations for the most pristine (uncontaminated) BSE-like rock group. In this same panel, the Zr and Hf scales have been set so that any vertical line has the chondritic value of  $\sim 37$  (Jochum et al., 1986).

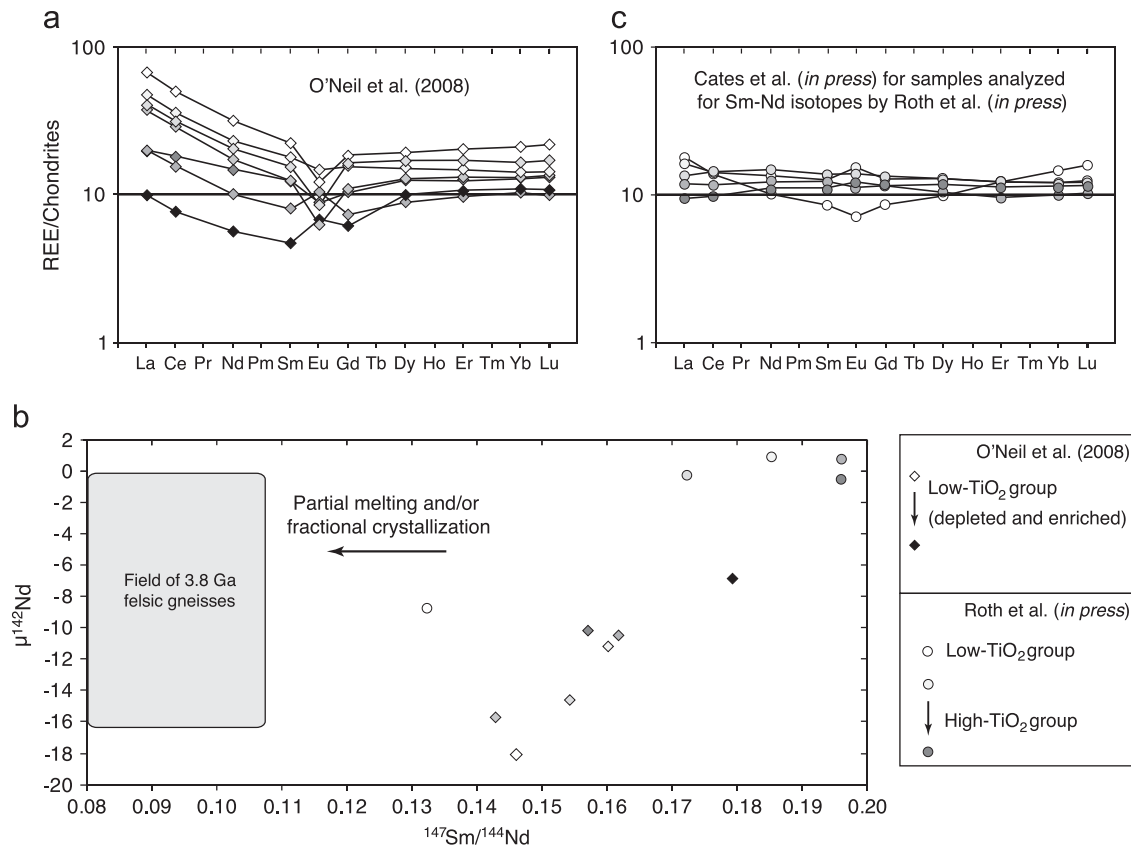


**Fig. 6.** Panel (a) shows chondrite-normalized (Sun and McDonough, 1989) REE patterns for the low- $\text{TiO}_2$  amphibolite samples of O'Neil et al. (2008). Panel (b) shows the relationship (positive correlation) between  $^{142}\text{Nd}$  anomalies and  $^{147}\text{Sm}/^{144}\text{Nd}$  for the samples of O'Neil et al. (2008) also presented in panel (a), and the samples of Roth et al. (*in press*). Panel (c) shows chondrite-normalized REE patterns, from Cates et al. (*in press*), which correspond to amphibolite samples analyzed for Sm–Nd isotopes by Roth et al. (*in press*). Note the large range of spectra in panel (a) ranging from light to middle REE depletion (black diamonds) to enrichment of light to heavy REE (white diamonds). This spectrum is also reflected in panel (b) where the global enrichment in REE (translated into the Sm/Nd ratio) seems to correlate with the size of  $^{142}\text{Nd}$  anomalies. Also shown is the field of isotopic compositions displayed by the felsic units in the Nuvvuagittuq supracrustal belt described as either TTG intrusive sheets (Cates and Mojzsis, 2007) or felsic bands (O'Neil et al., 2008). (c) illustrates the difference between high- $\text{TiO}_2$  relatively flat (grey shaded circles) and low- $\text{TiO}_2$  fractionated (white circles) REE patterns for rocks analyzed in this study.

(similar to the “high- $\text{TiO}_2$ ” group) have been documented in the NSB (Cates and Mojzsis, 2007) and the few samples of this kind analyzed for  $\mu^{142}\text{Nd}$  (O'Neil et al., 2008, 2012) have the closest-to-BSE, or slightly supra-BSE, compositions among the NSB rocks in both  $^{142}\text{Nd}/^{144}\text{Nd}$  and  $^{147}\text{Sm}/^{144}\text{Nd}$ .

The “low- $\text{TiO}_2$ ” group NSB amphibolites that carry negative  $^{142}\text{Nd}$  anomalies have REE patterns which resemble depleted peridotite that was later re-fertilized to yield subchondritic Sm/Nd ratios (O'Neil et al., 2011; Fig. 6). Even a “low- $\text{TiO}_2$ ”

amphibolite sample with the least re-fertilized REE pattern (sample PC-230 in O'Neil et al., 2008) has a  $^{142}\text{Nd}$  deficit of  $-6.8$ , which is consistent with its subchondritic Sm/Nd ratio. Data in Fig. 6 show that an increase of LREE compared to HREE (translated into an increase in La/Yb) is associated with larger  $^{142}\text{Nd}$  deficits, decreasing Sm/Nd, and an increase in total REE content. It is likely then that the  $^{142}\text{Nd}$  anomalies developed in the “low- $\text{TiO}_2$ ” mantle source of these amphibolites after re-fertilization rather than being acquired through contamination

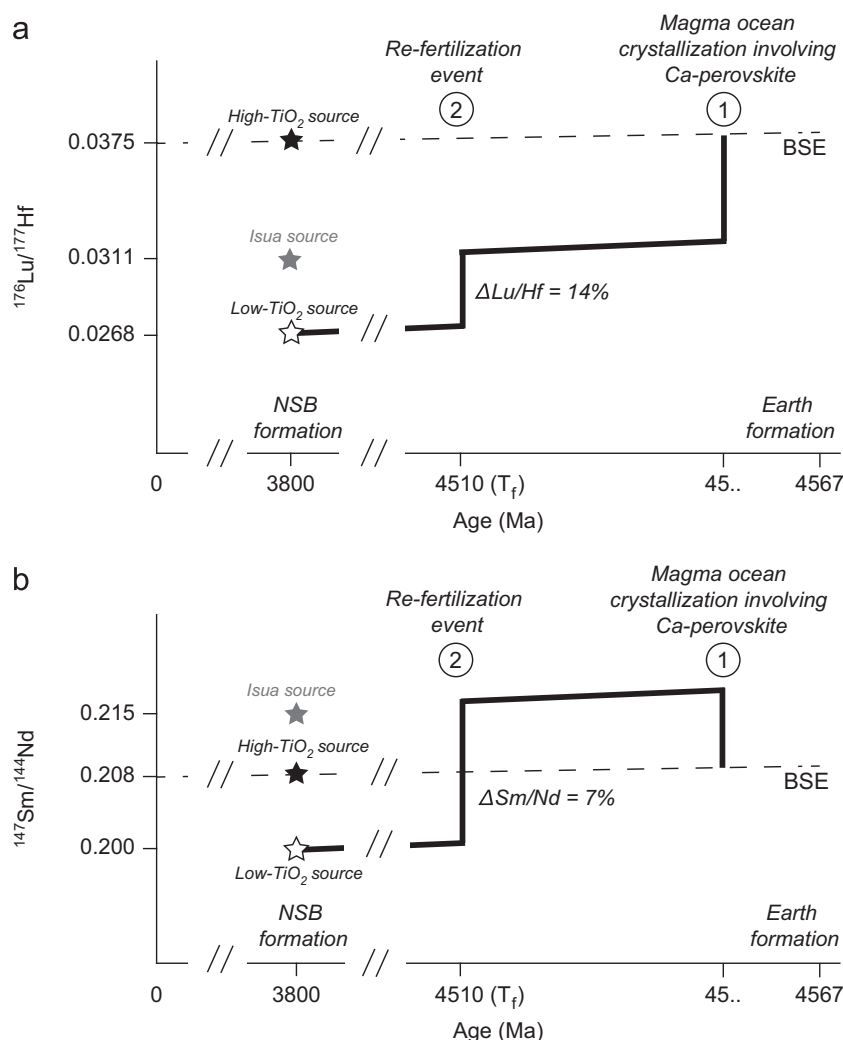


**Fig. 7.** Schematic  $^{176}\text{Lu}/^{177}\text{Hf}$  (a) and  $^{147}\text{Sm}/^{144}\text{Nd}$  (b) evolution diagrams showing the enriched mantle source history before the actual formation of the NSB at ca. 3800 Ma. In this model (see Section 4.4), the NSB mantle source first evolved with a BSE composition until it was fractionated during crystallization of a terrestrial magma ocean in the presence of Ca- and Mg-perovskite (event 1). It was then re-fertilized at  $T_f$  (4510 Ma corresponding to event 2) and subsequently evolved in a closed system to develop  $^{142}\text{Nd}$  anomalies until NSB formation. Also shown are the  $^{176}\text{Lu}/^{177}\text{Hf}$  and  $^{147}\text{Sm}/^{144}\text{Nd}$  values of the NSB high-TiO<sub>2</sub> amphibolite source together with the same parameters for the source of the Isua amphibolites (see text for more details). The BSE values were taken from Caro and Bourdon (2010). Note that the slopes of parent/daughter evolution through time are not to scale for the sake of clarity.

with an enriched reservoir. The “low-TiO<sub>2</sub>” source was already enriched, and even the least enriched amphibolites have Sm/Nd ratios below BSE. This episode of re-fertilization necessarily has to have occurred early in Earth history to be recorded in the form of  $^{142}\text{Nd}$  anomalies. Therefore, the conclusion is that the positive correlation between  $^{142}\text{Nd}/^{144}\text{Nd}$  and  $^{147}\text{Sm}/^{144}\text{Nd}$  stems from the combined effect of Hadean mantle re-fertilization and mixing between the “low-” (negative anomalies) and “high-TiO<sub>2</sub>” (BSE composition) amphibolite sources at the time the NSB was formed at ca. 3800 Ma. Later metamorphic events modified the apparent slope of Sm–Nd and Lu–Hf isochrons as detailed in Roth et al. (in press), while still preserving the mixing hyperbola (Fig. 4).

The inferred proportions of mixing between the hypothesized end-members are too substantial to match a scenario of straightforward contamination by later assimilation of one group by the other because the allowable limit of ~20% (Bohrson and Spera, 2001; Reiners et al., 1995) is exceeded (Fig. 4). This means that the two groups were contemporaneous magmas able to mix in high proportions, which in turn justifies the use of the scatterchron to determine an average age for the NSB rocks. The magma mixing processes assumed for the Nuvvuagittuq rocks are similar to those

commonly seen in recent magmatic provinces (Cantagrel et al., 1984), and also discussed in detail by Perugini and Poli (2012).

#### 4.3. Age of the re-fertilization event

An important parameter for understanding Earth’s early history is the age of the fractionation event that must have occurred in the Hadean in order to allow for the development of the observed  $^{142}\text{Nd}$  anomalies. As concluded in Section 4.2.2, the age derived from the correlation between  $^{142}\text{Nd}/^{144}\text{Nd}$  and  $^{147}\text{Sm}/^{144}\text{Nd}$  cannot date this event because it has been shifted towards a younger age (Roth et al., in press). Therefore, a solution must be found to a two-stage model that simultaneously solves for the initial  $^{143}\text{Nd}/^{144}\text{Nd}$ ,  $^{142}\text{Nd}/^{144}\text{Nd}$ , and  $^{176}\text{Lu}/^{177}\text{Hf}$  ratios, which corresponds to three unknowns (Sm/Nd, Lu/Hf, and the time of fractionation,  $T_f$ ). A least-squares equation was used to minimize the differences between the target and calculated values such that these differences do not exceed the analytical uncertainties and iteratively converge to the solution. In this model, it was assumed that the time spent between the depletion and later re-fertilization episodes corresponds to a single fractionation event to match a simple two-stage model. It was further

assumed that the silicate mantle before fractionation at  $T_f$  had a composition equivalent to that of the non-chondritic BSE of Caro and Bourdon (2010); this corresponds to the composition of the mantle after formation of a hidden reservoir or via collisional erosion (O'Neill and Palme, 2008). The decay constant of Kinoshita et al. (2012) was used for these new  $^{146}\text{Sm}$ – $^{142}\text{Nd}$  isotope system calculations. The best solution obtained by iteration gave 4510 Ma as the time of the fractionation event, while the derived result for  $^{147}\text{Sm}/^{144}\text{Nd}$  ( $\sim 0.20$ ) was only slightly lower than BSE, and  $^{176}\text{Lu}/^{177}\text{Hf}$  was equal to 0.0268 (see Fig. 7). This latter value is significantly below that of BSE.

#### 4.4. Early history of the enriched reservoir and possible link with worldwide $^{142}\text{Nd}$ anomalies

Although the exact re-fertilization protagonist(s) cannot be identified based on the present data, some useful observations can still be made. Prior to the re-fertilization event (estimated to take place around 4510 Ma), the mantle source that hosted  $^{142}\text{Nd}$  anomalies must have been significantly fractionated. Yet, the exact cause for fractionation remains unclear and probably corresponds to partial melting of a primitive mantle-like source.

As both positive and negative  $^{142}\text{Nd}$  anomalies have been reported for ancient terrestrial rocks that counterbalance each other to yield the BSE composition, it is legitimate to ask whether the two types of anomalies are genetically related or complementary. An interesting outcome of the model presented in Section 4.3 is that the fractionation followed by a re-fertilization event changed the mantle  $^{176}\text{Lu}/^{177}\text{Hf}$  ratio by 29% relative to BSE (0.0268), while the  $^{147}\text{Sm}/^{144}\text{Nd}$  ratio was changed by only 4% compared to BSE (0.200) as illustrated in Fig. 7. This incongruence between Lu/Hf and Sm/Nd cannot simply be explained by melt extraction or re-fertilization involving mineral assemblages that fractionate elements in ways similar to those of the ambient upper mantle. Therefore, as suggested by Caro et al. (2005), Hoffmann et al. (2011), and Rizo et al. (2011), the observed decoupling between the Sm–Nd and Lu–Hf isotope systems could instead originate from an earlier event of Ca- and Mg-perovskite fractionation in the lower mantle (note that the actual mode of Ca-perovskite would not need to be large, e.g. Caro et al., 2005), which would be consistent with the direction and amplitude of the observed Hf–Nd decoupling. To account for the decoupling in the NSB enriched source, it is assumed here that the mantle source prior to re-fertilization already had fractionated Lu/Hf and Sm/Nd ratios similarly to what is observed for the source of Isua amphibolites. The re-fertilization event hence would not have actually fractionated Sm/Nd relative to Lu/Hf but only lowered these ratios from the initially supra-BSE  $^{147}\text{Sm}/^{144}\text{Nd}$  and sub-BSE  $^{176}\text{Lu}/^{177}\text{Hf}$  ratios (Fig. 7). As a result, when calculating the time-integrated  $^{147}\text{Sm}/^{144}\text{Nd}$  and  $^{176}\text{Lu}/^{177}\text{Hf}$  ratios for the Isua amphibolite source (using the data of Rizo et al. (2011) for consistency between the two isotope systems) we find, respectively, 0.215 and 0.0311 (with the approach outlined in Section 4.3). If these ratios are compared to those inferred from the NSB enriched source, it follows that the re-fertilization event further fractionated the  $^{147}\text{Sm}/^{144}\text{Nd}$  and  $^{176}\text{Lu}/^{177}\text{Hf}$  ratios relative to the Isua amphibolite source by, respectively, 7% and 14%. These results are in accord with what would be expected as the outcome of a re-fertilization process. It seems that the Isua and Nuvvuagittuq amphibolite sources shared a common early history that may be linked to the consequences of crystallization of an early deep magma ocean, which is also consistent with the old age obtained for the value of  $T_f$  (Fig. 7). The NSB source possibly was located at shallower depths within the mantle than the ISB source and was affected by re-fertilization at ca. 4510 Ma; as a consequence, the histories of Isua and Nuvvuagittuq subsequently diverged.

## 5. Conclusions

This study presents new Lu–Hf isotope data for Eoarchean rocks from the Nuvvuagittuq supracrustal belt that integrates the data with other radiogenic systems (Sm–Nd, U–Pb) and trace element compositions of metavolcanic and metasedimentary rocks. Results indicate an emplacement age of  $3864 \pm 70$  Ma for the Nuvvuagittuq supracrustal belt (both mafic and felsic lithologies) that is in agreement with  $^{147}\text{Sm}$ – $^{143}\text{Nd}$  (David et al., 2009; O'Neil et al., 2008; Roth et al., in press) and zircon U–Pb ages (Cates and Mojzsis, 2007, 2009; Cates et al., in press; David et al., 2009). This age is best interpreted as the mean age of the different samples analyzed and not as a strict isochron because it is recognized that the analyzed samples are likely not co-genetic. The Nuvvuagittuq supracrustal belt, however, is old enough for its isotope compositions to be dominated by radiogenic ingrowth, which is sensitive to significant age variations. Hafnium and Nd isotope systematics calculated at 3800 Ma reveal a well-defined mixing hyperbola. This mixing event possibly took place between the protoliths of the two NSB amphibolite groups identified by O'Neil et al. (2011; cf. Cates et al., in press). Owing to a clear difference and some variability in the REE patterns of each group, one cannot derive one group from the other by simple assimilation of evolved Hadean crust. Such a scenario fails to explain the existence of  $^{142}\text{Nd}$  anomalies nor can it reconcile the correlation between these anomalies and the Sm/Nd ratios of NSB rocks. Furthermore, we conclude that the  $^{142}\text{Nd}$  anomalies were not acquired through contamination of each amphibolite group by the same enriched Hadean crust, but instead the anomalies are endemic to one of the two sources. The “low-TiO<sub>2</sub>” amphibolites (O'Neil et al., 2011) have the most pronounced  $^{142}\text{Nd}$  anomalies and always have Sm/Nd ratios lower than BSE. In addition, they have typical REE patterns of depleted mantle later re-fertilized in LREE with a large range of depletion and replenishment. We propose that the  $^{142}\text{Nd}$  anomalies developed in response to a re-fertilization process that happened in an already fractionated Hadean mantle source at 4510 Ma.

## Acknowledgments

We are grateful to Nicole Cates for help with technical matters and fieldwork and to Philippe Telouk for maintenance of the Lyon Nu Plasma. J.B.T. acknowledges financial support from the French Programme National de Planétologie of the Institut National des Sciences de l'Univers and Centre National d'Etudes Spatiales, and from the French Agence Nationale de la Recherche (Grants BEGDy—Birth and Evolution of Terrestrial GeoDynamics and M&Ms – Mantle Melting – Measurements, Models, Mechanisms). S.J.M. gratefully acknowledges logistical assistance for work in the Nuvvuagittuq supracrustal belt from the Pituvik Corporation of Nunavik (Québec), and financial support from the Laboratoire de Géologie de Lyon at Ecole Normale Supérieure de Lyon and Université Claude Bernard Lyon 1, the NASA Exobiology Program (Grant Exploring the Hadean Earth), the National Geographic Society, and the J. William Fullbright Foundation. This work was also supported by an ETH internal grant to B.B. We thank Klaus Mezger and Igor Puchtel for constructive reviews that helped improve the manuscript, and Bernard Marty for editorial handling.

## References

- Abati, J., Arenas, R., 2005. Metamorphic evolution of anthophyllite/cummingtonite-cordierite rocks from the upper unit of the Ordenes Complex (Galicia, NW Spain). *Eur. J. Mineral.* 17, 57–68.
- Arndt, N.T., 2008. *Komatiites*. Cambridge University Press, Cambridge.

- Bennett, V.C., 2007. Coupled  $^{142}\text{Nd}$ – $^{143}\text{Nd}$  isotopic evidence for Hadean mantle dynamics. *Science* 318, 1907–1910.
- Blichert-Toft, J., 2001. On the Lu–Hf isotope geochemistry of silicate rocks. *Geostand. Newslett.* 25, 41–56.
- Blichert-Toft, J., Boyet, M., Télouk, P., Albarède, F., 2002.  $^{147}\text{Sm}$ – $^{143}\text{Nd}$  and  $^{176}\text{Lu}$ – $^{176}\text{Hf}$  in eucrites and the differentiation of the HED parent body. *Earth Planet. Sci. Lett.* 204, 167–181.
- Blichert-Toft, J., Chauvel, C., Albarède, F., 1997. Separation of Hf and Lu for high-precision isotope analysis of rock samples by magnetic sector-multiple collector ICP-MS. *Contrib. Mineral. Petrol.* 127, 248–260.
- Blichert-Toft, J., Leshar, C.E., Rosing, M.T., 1992. Selectively contaminated magmas of the Tertiary East Greenland macrodike complex. *Contrib. Mineral. Petrol.* 110, 154–172.
- Bohrson, W.A., Spera, F.J., 2001. Energy-constrained open-system magmatic processes II: application of energy-constrained assimilation-fractional crystallization (EC-AFC) model to magmatic systems. *J. Petrol.* 42, 1019–1041.
- Bouvier, A., Vervoort, J.D., Patchett, P.J., 2008. The Lu–Hf and Sm–Nd isotopic composition of CHUR: constraints from unequilibrated chondrites and implications for the bulk composition of terrestrial planets. *Earth Planet. Sci. Lett.* 273, 48–57.
- Bowring, S.A., Williams, I.S., 1999. Priscoan (4.00–4.03 Ga) orthogneisses from northwestern Canada. *Contrib. Mineral. Petrol.* 134, 3–16.
- Boyet, M., Blichert-Toft, J., Rosing, M., Storey, M., Télouk, P., Albarède, F., 2003.  $^{142}\text{Nd}$  evidence for early Earth differentiation. *Earth Planet. Sci. Lett.* 214, 427–442.
- Boyet, M., Carlson, R.W., 2005.  $^{142}\text{Nd}$  evidence for early (> 4.53 Ga) global differentiation of the silicate Earth. *Science* 309, 576–581.
- Cantagrel, J.-M., Didier, J., Gourgaud, A., 1984. Magma mixing: origin of intermediate rocks and “enclaves” from volcanism to plutonism. *Phys. Earth Planet. Inter.* 35, 63–76.
- Caro, C., Bourdon, B., Birck, J.L., Moorbath, S., 2003.  $^{146}\text{Sm}$ – $^{142}\text{Nd}$  evidence from Isua metamorphosed sediments for early differentiation of the Earth's mantle. *Nature* 423, 428–432.
- Caro, G., 2011. Early silicate Earth differentiation. *Annu. Rev. Earth Planet. Sci.* 39, 31–58.
- Caro, G., Bourdon, B., 2010. Non-chondritic Sm/Nd ratio in the terrestrial planets: consequences for the geochemical evolution of the mantle–crust system. *Geochim. Cosmochim. Acta* 74, 3333–3349.
- Caro, G., Bourdon, B., Birck, J.-L., Moorbath, S., 2006. High-precision  $^{142}\text{Nd}/^{144}\text{Nd}$  measurements in terrestrial rocks: constraints on the early differentiation of the Earth's mantle. *Geochim. Cosmochim. Acta* 70, 164–191.
- Caro, G., Bourdon, B., Wood, B.J., Corgne, A., 2005. Trace-element fractionation in Hadean mantle generated by melt segregation from a magma ocean. *Nature* 436, 246–249.
- Cates, N.L., Mojzsis, S.J., 2007. Pre-3750 Ma supracrustal rocks from the Nuvvuagittuq supracrustal belt, northern Québec. *Earth Planet. Sci. Lett.* 255, 9–21.
- Cates, N.L., Mojzsis, S.J., 2009. Metamorphic zircon, trace elements and Neoproterozoic metamorphism in the ca. 3.75 Ga Nuvvuagittuq supracrustal belt, Québec (Canada). *Chem. Geol.* 261, 99–114.
- Cates, N.L., Ziegler, K., Schmitt, A.K., Mojzsis, S.J. Reduced, reused and recycled: detrital zircons of the 3780 Myr-old Nuvvuagittuq supracrustal belt (Québec, Canada). *Earth Planet. Sci. Lett.*, <http://dx.doi.org/10.1016/j.epsl.2012.11.054>, in press.
- Chase, C.G., Patchett, P.J., 1988. Stored mafic/ultramafic crust and early Archean mantle depletion. *Earth Planet. Sci. Lett.* 91, 66–72.
- Compston, W., Pidgeon, R.T., 1986. Jack Hills, evidence of more very old detrital zircons in Western Australia. *Nature* 321, 766–769.
- David, J., Godin, L., Stevenson, R., O'Neil, J., Francis, D., 2009. U–Pb ages (3.8–2.7 Ga) and Nd isotope data from the newly identified Eoarchean Nuvvuagittuq supracrustal belt, Superior craton, Canada. *Geol. Soc. Am. Bull.* 121, 150–163.
- David, J., Parent, M., Stevenson, R.K., Nadeau, P., Godin, L., 2002. La séquence supracrustale de Porpoise Cove, région d'Inukjuak; un exemple unique de croûte paléo-archéenne (ca. 3.8 Ga) dans la Province du Supérieur. *Ministère des Ressources naturelles, Québec DV-2002*, pp. 10–17.
- Duchêne, S., Blichert-Toft, J., Luais, B., Télouk, P., Lardeaux, J.-M., Albarède, F., 1997. The Lu–Hf dating of garnets and the ages of the Alpine high-pressure metamorphism. *Nature* 387, 586–589.
- Froude, D.O., Ireland, T.R., Kinny, P.D., Williams, I.S., Compston, W., Williams, I.R., Myers, J.S., 1983. Ion microprobe identification of 4100–4200 Myr-old terrestrial zircons. *Nature* 304, 616–618.
- Guitreau, M., Blichert-Toft, J., Martin, H., Mojzsis, S.J., Albarède, F., 2012. Hafnium isotope evidence from Archean granitic rocks for deep mantle origin of continental crust. *Earth Planet. Sci. Lett.* 337–338, 211–223.
- Harrison, M.T., 2009. The Hadean crust: evidence from > 4 Ga zircons. *Annu. Rev. Earth Planet. Sci.* 37, 479–505.
- Herwartz, D., Nagel, T.J., Münker, C., Scherer, E.E., Froitzheim, N., 2011. Tracing two orogenic cycles in one eclogite sample by Lu–Hf garnet chronometry. *Nat. Geosci.* 4, 178–183.
- Hoffmann, E.J., Münker, C., Polat, A., M.T. R., Schulz, T., 2011. The origin of decoupled Hf–Nd isotope compositions in Eoarchean rocks from southern West Greenland. *Geochim. Cosmochim. Acta* 75, 6610–6628.
- Hopkins, M., Harrison, M.T., Manning, C.E., 2008. Low heat flow inferred from > 4 Gyr zircons suggests Hadean plate boundary interactions. *Nature* 456, 493–496.
- Hoskin, P.W.O., Schaltegger, U., 2003. The composition of zircon and igneous and metamorphic petrogenesis. *Zircon*, 27–62.
- Jochum, K.P., Seufert, H.M., Spettel, B., Palme, H., 1986. The solar-system abundances of Nb, Ta and Y, and the relative abundance of refractory lithophile elements in differentiated planetary bodies. *Geochim. Cosmochim. Acta* 50, 1173–1183.
- Kemp, A.I.S., Wilde, S.A., Hawkesworth, C.J., Coath, C.D., Nemchin, A., Pidgeon, R.T., Vervoort, J.D., DuFrane, S.A., 2010. Hadean crustal evolution revisited: new constraints from Pb–Hf isotope systematics of the Jack Hills zircons. *Earth Planet. Sci. Lett.* 296, 45–56.
- Kinoshita, N., Paul, M., Kashiv, Y., Collon, P., Deibel, C.M., DiGiovine, B., Greene, J.P., Henderson, D.J., Jiang, C.L., Marley, S.T., Nakanishi, T., Pardo, R.C., Rehm, K.E., Robertson, D., Scott, R., Schmitt, C., Tang, X.D., Vondrasek, R., Yokoyama, A., 2012. A shorter  $^{146}\text{Sm}$  half-life measured and implications for  $^{146}\text{Sm}$ – $^{142}\text{Nd}$  chronology in the solar system. *Science* 335, 1614–1617.
- Kohn, M.J., Spear, F.S., Valley, J.W., 1997. Dehydration-melting and fluid recycling during metamorphism: Rangeley formation, New Hampshire, USA. *J. Petrol.* 38, 1255–1277.
- Langmuir, C.H., Vocke Jr., R.D., Hanson, G.N., 1978. A general mixing equation with applications to Icelandic basalts. *Earth Planet. Sci. Lett.* 37, 380–392.
- Ludwig, K.R., 2008. User's manual for Isoplot 3.6: a geochronological toolkit for Microsoft Excel. Berkeley Geochronology Center Special Publication. 4.
- Maier, A.C., Cates, N.L., Trail, D., Mojzsis, S.J., 2012. Geology, age and field relations of Hadean zircon-bearing supracrustal rocks from Quad Creek, eastern Beartooth Mountains (Montana and Wyoming, USA). *Chem. Geol.* 312–313, 47–57.
- Mojzsis, S.J., Harrison, T.M., Pidgeon, R.T., 2001. Oxygen-isotope evidence from ancient zircons for liquid water at the Earth's surface 4300 Myr ago. *Nature* 409, 178–181.
- O'Neil, J., Carlson, R.W., Francis, D., Stevenson, R.K., 2008. Neodymium-142 evidence for Hadean mafic crust. *Science* 321, 1828–1831.
- O'Neil, J., Carlson, R.W., Paquette, J.L., Francis, D., 2012. Formation age and metamorphic history of the Nuvvuagittuq Greenstone Belt. *Precambrian Res.* 220–221, 23–44.
- O'Neil, J., Francis, D., Carlson, R.W., 2011. Implications of the Nuvvuagittuq greenstone belt for the formation of Earth's early crust. *J. Petrol.* 52, 985–1009.
- O'Neill, H.S.C., Palme, H., 2008. Collisional erosion and the non-chondritic composition of the terrestrial planets. *Philos. Trans. R. Soc. London A* 366, 4205–4238.
- Perugini, D., Poli, G., 2012. The mixing of magmas in plutonic and volcanic environments: analogies and differences. *Lithos* 153, 261–277.
- Reiners, P.W., Nelson, B.K., Ghiorso, M.S., 1995. Assimilation of felsic crust by basaltic magma: thermal limits and extents of crustal contamination of mantle-derived magmas. *Geology* 23, 563–566.
- Rizo, H., Boyet, M., Blichert-Toft, J., Rosing, M., 2011. Combined Nd and Hf isotope evidence for deep-seated source of Isua lavas. *Earth Planet. Sci. Lett.* 312, 267–279.
- Roth, A., Bourdon, B., Mojzsis, S.J., Touboul, M., Sprung, P., Guitreau, M., Blichert-Toft, J. Inherited  $^{142}\text{Nd}$  anomalies in Eoarchean protoliths. *Earth Planet. Sci. Lett.*, <http://dx.doi.org/10.1016/j.epsl.2012.11.023>, in press.
- Sullivan, N.C., Baxter, E.F., Mojzsis, S.J., 2011. 2575 Ma age of Nuvvuagittuq metamorphic garnet. In: *Proceedings of the V.M. Goldschmidt Conference, Prague*.
- Sun, S.S., McDonough, W.F., 1989. Chemical and isotopic systematics of oceanic basalts; implications for mantle composition and processes. In: Saunders, A.D., Norry, M.J. (Eds.), *Magmatism in the Ocean Basins*. Geological Society Special Publication, London, pp. 313–345.
- Trail, D., Watson, B.E., Tailby, N.D., 2011. The oxidation state of Hadean magmas and implications for early Earth's atmosphere. *Nature* 480, 79–83.